Dynamic Stresses and Displacements around Cylindrical Cavities in an Infinite Elastic Medium under Moving Step Loads on the Cavity's Surface

Hamid Mohsenimonfared [1], M. Nikkhahbahrami [2]

[1.] Department of mechanical Engineering, Science & Research Branch, Islamic Azad University (IAU), Tehran, Iran
[2.] Department of mechanical Engineering, Tehran University, Tehran, Iran
h-mohsenimonfared@iau-arak.ac.ir

Abstract: Potential functions and Fourier series method in the cylindrical coordinate system are employed to solve the problem of moving loads on the surface of a cylindrical bore in an infinite elastic medium. The steady-state dynamic equations of medium are uncoupled into Helmholtz equations, via given potentials. It is used that because of the superseismic nature of the problem, two mach cones are formed and opened toward the rear of the front in the medium. The stresses and displacements are obtained by using integral equations with certain boundary conditions. Finally, the dynamic stresses and displacements for step loads with axisymmetric and nonaxisymmetric cases are obtained and discussed in details via a numerical example. Moreover, effects of Mach numbers and poisson's ratio of medium on the values of stresses are discussed.

[Hamid Mohsenimonfared, M.Nikkhahbahrami. **Dynamic Stresses and Displacements around Cylindrical Cavities in an Infinite Elastic Medium under Moving Step Loads on the Cavity's Surface.** *Life Sci J* 2015;12(9):55-66]. (ISSN:1097-8135). http://www.lifesciencesite.com. 7

Keywords: Wave propagation, Fourier series method, cylindrical cavities, Helmholtz equations, moving load.

1. Introduction

1.1 General Remarks

Moving loads on the surfaces have been investigated by many researchers. Investigation on dynamic stresses in solids is very significant in the study of dynamic strength of materials and in the design of underground structures subject to ground blasting waves. A related but considerably simpler problem has been treated by Biot (1952), who considered space- harmonic axisymmetric standing waves and obtained a closed form solution. Another related problem was treated by Cole and Huth (1958), who considered a line load progressing with a velocity V on the surface of an elastic half- space. Because of the simpler geometry, they were able to obtain a solution in closed form. Adrianus (2002) investigated the moving point load problem in soil dynamics with a view to determine the ground motion generated by a high-speed train traveling on a poorly consolidated soil with low shear wave speed. M.C.M. Bakker (1999) revisited the nonaxisymmetrical boundary value problem of a point load of normal traction traveling over an elastic half-space. M. Rahman (2001) considered the problem of a line load moving at a constant transonic speed across the surface of an elastic half-space and derived solution of the problem by using the method of Fourier transform. Iavorskaia (1964) also studied diffraction of a plane longitudinal wave on circular cylinder. One basic method has been used for the solution of these problems, the solution is obtained by using an integral transform of the displacement potentials. The resulting transformed equations are then solved in terms of Hankel functions, and finally the stresses and displacements are found by inversion of the transformed quantities. In this paper the coefficients of the stresses and displacements are found by solving sets of coupled integral equations.

The waves are expanded into Fourier series in terms of the angle, θ , around the opening. The stress field of the wave is written in terms of potential functions which satisfy the equations of motion. These equations decoupled via introducing the potential functions and reduced to Helmholtz equations that the potentials satisfy.

These potential functions are in integral form with unknown functions in the integrands. Therefore the Fourier series coefficients of the stresses and displacements are also in integral form with unknown integrands. The applied boundary tractions (the step loads) are expanded into a Fourier series in θ and expressions for the stress and displacement components at points in the medium are derived for each term of the Fourier series as functions of the radial distance r from the cavity axis and the distance z behind the wave front.

The following three cases of step loads are considered: normal to the surface, tangential to the surface in the direction of the axis of the bore, and tangential to the circle of load application. These results can be used, by superposition, to determine the effects of other load patterns moving with the velocity V in the direction of the axis of the bore.

Numerical solution of these equations gives the values of the unknown functions. These values can

then be used to find the stresses and displacements on the boundary and also anywhere in the medium.

1.2 Problem Description

The object of this work is to obtain stresses and displacements in an elastic medium in the vicinity of a cylindrical cavity which is engulfed by a plane stress wave of dilatational travelling parallel to the axis of the cylinder, as shown in Figure 1.

The step load has an arbitrary distribution $P(\theta)$ along the circumference of the circle and moves with a velocity $V > C_1 > C_2$; therefore, the speed is superseismic with respect to both the dilatational and shear waves in the medium. Consequently, the disturbances which were initiated far behind the front on the boundary of the cavity cannot reach the vicinity of the wave front for some time after the incident wave passes.

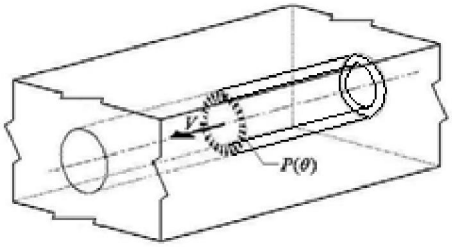

Figure 1. Moving step load

Moreover, because of the super seismic nature of the problem, it should be expected that two mach cones will be formed in the medium, as shown in Figure 2. These cones should open toward the rear of the front. Furthermore, there can be no stresses or displacements ahead of the leading front.

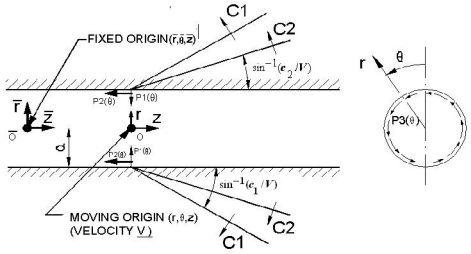

Figure 2. Geometry of the problem and the coordinate systems

If a coordinate system is assumed to move along the cylinder with the wave front, it is seen that the state of stress at points close behind the wave front depends only on relative position of them with respect to the front. Thus, in the vicinity of the wave front, provided that the end of the cavity is far away, the problem may be treated as a steady-state case. In other words, in the moving coordinate system, the state of stress and displacement is independent of time.

2. Governing equations and general solutions

Consider a cylindrical cavity of radius r = a in a linearly elastic, homogeneous, and isotropic medium referred to a fixed coordinate system $(\bar{r}, \bar{\theta}, \bar{z})$ whose origin lies on the axis of the cavity.

A step load along the circle at $\bar{z}$ = -vt progresses along the interior of the cavity with a velocity V such that the stresses on the boundary r=a are:

$$\sigma_{rr}\Big|_{r=a} = \sigma_1(\bar{\theta})U(\bar{z}+vt) \quad (1)$$

$$\sigma_{r\theta}\Big|_{r=a} = \sigma_2(\bar{\theta})U(\bar{z}+vt) \quad (2)$$

$$\sigma_{rz}\Big|_{r=a} = \sigma_3(\bar{\theta})U(\bar{z}+vt) \quad (3)$$

Where the functions $\sigma_k(\theta\theta)$ define the distribution of the applied load. To determine the steady state solution, a moving coordinate system (r, θ ,z) is introduced such that:

$$r = \bar{r}, \theta = \bar{\theta}, z = \bar{z} + Vt \quad (4)$$

The following treatment is restricted to the case where the velocity V is greater than C_1 and C_2, the respective propagation velocities of dilatational and equivoluminal waves in the medium. Hence

$$M_1 = \frac{V}{C_1} > 1, \quad M_2 = \frac{V}{C_2} > 1 \quad (5)$$

Where

$$C_1 = \sqrt{\frac{\lambda + 2\mu}{\rho}}, \quad C_2 = \sqrt{\frac{\mu}{\rho}} \quad (6)$$

The equations of motion in cylindrical coordinates, r, θ, z, for an elastic medium, may be expressed in the following form:

$$\begin{aligned}
&\nabla^2 u_r - \frac{1}{r^2}(u_r + 2\frac{\partial u_\theta}{\partial \theta}) + (\frac{\lambda}{\mu}+1)\frac{\partial \Delta}{\partial r} = \frac{\rho}{\mu}\frac{\partial^2 u_r}{\partial t^2} \\
&\nabla^2 u_\theta - \frac{1}{r^2}(u_\theta - 2\frac{\partial u_r}{\partial \theta}) + (\frac{\lambda}{\mu}+1)\frac{1}{r}\frac{\partial \Delta}{\partial \theta} = \frac{\rho}{\mu}\frac{\partial^2 u_\theta}{\partial t^2} \\
&\nabla^2 u_{\bar{z}} + (\frac{\lambda}{\mu}+1)\frac{\partial \Delta}{\partial \bar{z}} = \frac{\rho}{\mu}\frac{\partial^2 u_{\bar{z}}}{\partial t^2}
\end{aligned} \quad (7)$$

Where the dilatation, Δ , and the laplacian operator, ∇^2 , are given by:

$$\begin{aligned}
\Delta &= \frac{\partial u_r}{\partial r} + \frac{u_r}{r} + \frac{1}{r}\frac{\partial u_\theta}{\partial \theta} + \frac{\partial u_{\bar{z}}}{\partial \bar{z}} \\
\nabla^2 &= \frac{\partial^2}{\partial r^2} + \frac{1}{r}\frac{\partial}{\partial r} + \frac{1}{r^2}\frac{\partial^2}{\partial \theta^2} + \frac{\partial^2}{\partial \bar{z}^2}
\end{aligned} \quad (8)$$

As mentioned earlier, the assumption of the existence of a steady-state case and trans-formation form r, θ , $\bar{z}$ coordinates to r, θ , z results in elimination of the time variable, t, from the equations of motion. This transformation is performed by the following relations, as given in relations (4):

$$z = \bar{z} + Vt$$

$$\frac{\partial}{\partial \bar{z}} = \frac{\partial}{\partial z}, \quad \frac{\partial}{\partial t} = V\frac{\partial}{\partial z}$$

Therefore equations (7) may be expressed as follows:

$$\begin{aligned}
&\nabla^2 u_r - \frac{1}{r^2}(u_r + 2\frac{\partial u_\theta}{\partial \theta}) + (\frac{\lambda}{\mu}+1)\frac{\partial \Delta}{\partial r} = \frac{\rho}{\mu}V^2\frac{\partial^2 u_r}{\partial z^2}\\
&\nabla^2 u_\theta - \frac{1}{r^2}(u_\theta - 2\frac{\partial u_r}{\partial \theta}) + (\frac{\lambda}{\mu}+1)\frac{1}{r}\frac{\partial \Delta}{\partial \theta} = \frac{\rho}{\mu}V^2\frac{\partial^2 u_\theta}{\partial z^2} \qquad (9)\\
&\nabla^2 u_z + (\frac{\lambda}{\mu}+1)\frac{\partial \Delta}{\partial_z} = \frac{\rho}{\mu}V^2\frac{\partial^2 u_z}{\partial z^2}
\end{aligned}$$

Stress components are given by

$$\begin{aligned}
\sigma_{rr} &= \lambda\Delta + 2\mu\frac{\partial u_r}{\partial r}\\
\sigma_{\theta\theta} &= \lambda\Delta + 2\mu(\frac{u_r}{r} + \frac{1}{r}\frac{\partial u_\theta}{\partial \theta})\\
\sigma_{zz} &= \lambda\Delta + 2\mu\frac{\partial u_z}{\partial z} \qquad (10)\\
\sigma_{r\theta} &= \mu(\frac{1}{r}\frac{\partial u_r}{\partial \theta} - \frac{u_\theta}{r} + \frac{\partial u_\theta}{\partial r})\\
\sigma_{rz} &= \mu(\frac{\partial u_r}{\partial z} + \frac{\partial u_z}{\partial r})\\
\sigma_{\theta z} &= \mu(\frac{\partial u_\theta}{\partial z} + \frac{1}{r}\frac{\partial u_z}{\partial \theta})
\end{aligned}$$

Displacement components u_r, u_θ and u_z may be expressed in Fourier series:

$$\begin{aligned}
u_r(r,\theta,z) &= \sum_{n=0}^{\infty} u_{n,r}(r,z)\cos n\theta\\
u_\theta(r,\theta,z) &= \sum_{n=1}^{\infty} u_{n,\theta}(r,z)\sin n\theta \qquad (11)\\
u_z(r,\theta,z) &= \sum_{n=0}^{\infty} u_{n,z}(r,z)\cos n\theta
\end{aligned}$$

Three potential functions are now introduced,

$$\begin{aligned}
\varphi(r,\theta,z) &= \sum_{n=0}^{\infty} \varphi_n(r,z)\cos n\theta\\
\psi(r,\theta,z) &= \sum_{n=0}^{\infty} \psi_n(r,z)\cos n\theta \qquad (12)\\
\chi(r,\theta,z) &= \sum_{n=1}^{\infty} \chi_n(r,z)\sin n\theta
\end{aligned}$$

The displacement components $u_{n,r}, u_{n,\theta}$ and $u_{n,z}$ are defined as follows:

$$\begin{aligned}
u_{n,r} &= \frac{\partial \varphi_n}{\partial r} + \frac{\partial^2 \psi_n}{\partial r \partial z} + \frac{n}{r}\chi_n\\
u_{n,\theta} &= -\frac{n}{r}\varphi_n - \frac{n}{r}\frac{\partial \psi_n}{\partial z} - \frac{\partial \chi_n}{\partial r} \qquad (13)\\
u_{n,z} &= \frac{\partial \varphi_n}{\partial z} - \left(\frac{\partial^2}{\partial r^2} + \frac{1}{r}\frac{\partial}{\partial r} - \frac{n^2}{r^2}\right)\psi_n
\end{aligned}$$

These equations may be obtained from the vector equation

$$\bar{u} = \text{grad}\varphi + \text{curl}\bar{\omega}$$

Where $\bar{\omega}$ is the sum of two independent vectors as follows:

$$\bar{\omega} = \bar{\chi} + \text{curl}\bar{\psi}$$

The vectors $\bar{\chi}$ and $\bar{\psi}$ have only one non- zero component which is in the z- direction in both cases.

$$\begin{aligned}
\chi_r &= 0 \qquad \psi_r = 0\\
\chi_\theta &= 0 \qquad \psi_\theta = 0\\
\chi_z &= \chi \qquad \psi_z = \psi
\end{aligned}$$

By substitution of the values given in equations (13) into the equations (9), it can be shown that the potential functions satisfy the modified wave equations.

$$\begin{aligned}
\nabla^2 \varphi_n &= (\frac{V}{c_1})^2\frac{\partial^2 \varphi_n}{\partial z^2}\\
\nabla^2 \psi_n &= (\frac{V}{c_2})^2\frac{\partial^2 \psi_n}{\partial z^2} \qquad (14)\\
\nabla^2 \chi_n &= (\frac{V}{c_2})^2\frac{\partial^2 \chi_n}{\partial z^2}
\end{aligned}$$

Stress components are expressed in Fourier series form as follows:

$$\begin{aligned}
\sigma_{rr}(r,\theta,z) &= \sum_{n=0}^{\infty} \sigma_{n,rr}(r,z)\cos n\theta\\
\sigma_{\theta\theta}(r,\theta,z) &= \sum_{n=0}^{\infty} \sigma_{n,\theta\theta}(r,z)\cos n\theta\\
\sigma_{zz}(r,\theta,z) &= \sum_{n=0}^{\infty} \sigma_{n,zz}(r,z)\cos n\theta\\
\sigma_{r\theta}(r,\theta,z) &= \sum_{n=1}^{\infty} \sigma_{n,r\theta}(r,z)\sin n\theta \qquad (15)\\
\sigma_{rz}(r,\theta,z) &= \sum_{n=0}^{\infty} \sigma_{n,rz}(r,z)\cos n\theta\\
\sigma_{\theta z}(r,\theta,z) &= \sum_{n=1}^{\infty} \sigma_{n,\theta z}(r,z)\sin n\theta
\end{aligned}$$

Equations (11) and (15) may be substituted into equations (10), and as a result stress- displacement relations may be written for each term of the series:

$$\sigma_{n,rr} = \lambda\Delta + 2\mu\frac{\partial u_{n,r}}{\partial r} \qquad (16)$$

$$\sigma_{n,\theta\theta}=\lambda\Delta+2\mu\left(\frac{u_{n,r}}{r}+n\frac{u_{n,\theta}}{r}\right)$$

$$\sigma_{n,zz}=\lambda\Delta+2\mu\frac{\partial u_{n,z}}{\partial z}$$

$$\sigma_{n,r\theta}=\mu\left(-n\frac{u_{n,r}}{r}-\frac{u_\theta}{r}+\frac{\partial u_{n,\theta}}{\partial r}\right)$$

$$\sigma_{n,rz}=\mu\left(\frac{\partial u_{n,r}}{\partial z}+\frac{\partial u_{n,z}}{\partial r}\right)$$

$$\sigma_{n,\theta z}=\mu\left(\frac{\partial u_{n,\theta}}{\partial z}-n\frac{u_{n,z}}{r}\right)$$

where

$$\Delta=\frac{\partial u_{n,r}}{\partial r}+\frac{u_{n,r}}{r}+n\frac{u_{n,\theta}}{r}+\frac{\partial u_{n,z}}{\partial z}$$

Substitution of equations (13) into equations (16) and application of the differential equations (14) result in the following equations for stress components:

$$\frac{a^2\sigma_{n,rr}}{\mu}=\left(M_2^2-2M_1^2\right)\varphi_{n,ZZ}+2\varphi_{n,RR}+2\psi_{n,RRZ}+\frac{2n}{R}\left(\chi_{n,R}-\frac{1}{R}\chi_n\right)$$

$$\frac{a^2\sigma_{n,\theta\theta}}{\mu}=\left(M_2^2-2\right)\varphi_{n,ZZ}-2\varphi_{n,RR}+\frac{2}{R}\left(\psi_{n,RZ}-\frac{n^2}{R}\psi_{n,Z}\right)-\frac{2n}{R}\left(\chi_{n,R}-\frac{1}{R}\chi_n\right)$$

$$\frac{a^2\sigma_{n,zz}}{\mu}=\left(M_2^2-2M_1^2+2\right)\varphi_{n,ZZ}-2\left(M_2^2-1\right)\psi_{n,ZZZ}$$

$$\frac{a^2\sigma_{n,r\theta}}{\mu}=-\frac{2n}{R}\left(\varphi_{n,R}-\frac{1}{R}\varphi_n\right)-\frac{2n}{R}\left(\psi_{n,RZ}-\frac{1}{R}\psi_{n,Z}\right)+\left(M_2^2-1\right)\chi_{n,ZZ}-2\chi_{n,RR} \quad (17)$$

$$\frac{a^2\sigma_{n,rz}}{\mu}=2\varphi_{n,RZ}-\left(M_2^2-2\right)\psi_{n,RZZ}+\frac{n}{R}\chi_{n,Z}$$

$$\frac{a^2\sigma_{n,\theta z}}{\mu}=-\frac{2n}{R}\varphi_{n,Z}+\left(M_2^2-2\right)\frac{n}{R}\psi_{n,ZZ}-\chi_{n,RZ}$$

Where the second set of subscripts of φ_n,ψ_n and χ_n represent the partial derivatives of these functions. R and Z are the dimensionless variables form:

$$R=\frac{r}{a},\ Z=\frac{z}{a} \quad (18)$$

The values M_1 and M_2 are defined as follows:

$$M_1=\frac{V}{C_1},\ M_2=\frac{V}{C_2}$$

Let (19)

$$\beta_1^2=M_1^2-1 \quad , \quad \beta_2^2=M_2^2-1$$

The differential equations (14) may be written in the following form:

$$\frac{\partial^2\varphi_n}{\partial R^2}+\frac{1}{R}\frac{\partial\varphi_n}{\partial R}-\frac{n^2}{R^2}\varphi_n=\beta_1^2\frac{\partial^2\varphi_n}{\partial Z^2}$$

$$\frac{\partial^2\psi_n}{\partial R^2}+\frac{1}{R}\frac{\partial\psi_n}{\partial R}-\frac{n^2}{R^2}\psi_n=\beta_2^2\frac{\partial^2\psi_n}{\partial Z^2} \quad (20)$$

$$\frac{\partial^2\chi_n}{\partial R^2}+\frac{1}{R}\frac{\partial\chi_n}{\partial R}-\frac{n^2}{R^2}\chi_n=\beta_2^2\frac{\partial^2\chi_n}{\partial Z^2}$$

It is seen that these equations have the same general form as the differential equations of the cylindrical waves obtained in reference (13). Therefore solutions of equations (20) may be obtained in a manner similar to that in reference (13). These solutions are given in integral form as follows (see Appendix A for verification of the solutions):

$$\varphi_n=\int_0^\infty f_n(Z-R\beta_1\cosh u)\cosh nu\,du$$

$$\psi_n=\int_0^\infty g_n(Z-R\beta_2\cosh u)\cosh nu\,du \quad (21)$$

$$\chi_n=\int_0^\infty h_n(Z-R\beta_2\cosh u)\cosh nu\,du$$

From consideration of the fact that the disturbances are zero ahead of the wave front, it is seen that the functions f_n, g_n and h_n are zero for the values of their arguments less than $-R\beta_1$, $-R\beta_2$ and $-R\beta_2$, respectively.

Therefore the upper limits of the integrals may be changed from ∞ to the following values:

$$u_1=\cosh^{-1}\left(1+\frac{Z}{R\beta_1}\right) \quad \text{for } \varphi_n$$

$$u_2=\cosh^{-1}\left(1+\frac{Z}{R\beta_2}\right) \quad \text{for } \psi_n \text{ \& } \chi_n \quad (22)$$

The integrals are then written with these limits:

$$\varphi_n=\int_0^{u_1} f_n\left(Z-R\beta_1\cosh u\right)\cosh nu\,du$$

$$\psi_n=\int_0^{u_2} g_n\left(Z-R\beta_2\cosh u\right)\cosh nu\,du \quad (23)$$

$$\chi_n=\int_0^{u_2} h_n\left(Z-R\beta_2\cosh u\right)\cosh nu\,du$$

3. Expressions of stresses and displacements

Substitution of equations (23) into equations (17) gives the following expressions for stress components.

$$\frac{a^2\sigma_{n,rr}}{\mu} = \int_0^{u_1} f''(\eta_1)[M_2^2 - 2 + 2\beta_1^2\sinh^2 u]\cosh nu\, du + 2\beta_2^2\int_0^{u_2} g'''(\eta_2)\cosh^2 u\cosh nu\, du - \beta_2^2\int_0^{u_2} h''(\eta_2)\sinh 2u\cosh nu\, du \quad (24a)$$

$$\frac{a^2\sigma_{n,\theta\theta}}{\mu} = \int_0^{u_1} f''(\eta_1)[M_2^2 - 2\beta_1^2\cosh^2 u]\cosh nu\, du - 2\beta_2^2\int_0^{u_2} g'''(\eta_2)\sinh^2 u\cosh nu\, du + \beta_2^2\int_0^{u_2} h''(\eta_2)\sinh 2u\cosh nu\, du \quad (24b)$$

$$\frac{a^2\sigma_{n,zz}}{\mu} = (M_2^2 - 2M_1^2 + 2)\int_0^{u_1} f''(\eta_1)\cosh nu\, du - 2\beta_2^2\int_0^{u_2} g'''(\eta_2)\cosh nu\, du \quad (24c)$$

$$\frac{a^2\sigma_{n,r\theta}}{\mu} = \beta_1^2\int_0^{u_1} f''(\eta_1)\sinh 2u\sinh nu\, du + \beta_2^2\int_0^{u_2} g'''(\eta_2)\sinh 2u\sinh nu\, du - \beta_2^2\int_0^{u_2} h''(\eta_2)\cosh 2u\cosh nu\, du \quad (24d)$$

$$\frac{a^2\sigma_{n,rz}}{\mu} = -2\beta_1\int_0^{u_1} f''(\eta_1)\cosh u\cosh nu\, du + \beta_2(M_2^2 - 2)\int_0^{u_2} g'''(\eta_2)\cosh u\cosh nu\, du + \beta_2\int_0^{u_2} h''(\eta_2)\sinh u\sinh nu\, du \quad (24e)$$

$$\frac{a^2\sigma_{n,\theta z}}{\mu} = -2\beta_1\int_0^{u_1} f''(\eta_1)\sinh u\sinh nu\, du + \beta_2(M_2^2 - 2)\int_0^{u_2} g'''(\eta_2)\sinh u\sinh nu\, du + \beta_2\int_0^{u_2} h''(\eta_2)\cosh u\cosh nu\, du \quad (24f)$$

Substitution of equations (23) into equations (13) gives the following expressions for displacement components,

$$\frac{\mu u_{n,r}}{a} = \frac{-R\beta_1^2}{n^2-1}\int_0^{u_1} f''(\eta_1)\sinh u\,[n\sinh nu\cosh u - \sinh u\cosh nu]\, du + \frac{-R\beta_2^2}{n^2-1}\int_0^{u_2} g'''(\eta_2)\sinh u\,[n\sinh nu\cosh u - \sinh u\cosh nu]\, du + \frac{-R\beta_2^2}{n^2-1}\int_0^{u_2} h''(\eta_2)\sinh u\,[\sinh nu\cosh u - n\sinh u\cosh nu]\, du \quad (25a)$$

$$\frac{\mu u_{n,\theta}}{a} = \frac{-R\beta_1^2}{n^2-1}\int_0^{u_1} f''(\eta_1)\sinh u\,[n\sinh u\cosh nu - \sinh nu\cosh u]\, du + \frac{-R\beta_2^2}{n^2-1}\int_0^{u_2} g'''(\eta_2)\sinh u\,[n\sinh u\cosh nu - \sinh nu\cosh u]\, du + \frac{R\beta_2^2}{n^2-1}\int_0^{u_2} h''(\eta_2)\sinh u[n\sinh nu\cosh u - \sinh u\cosh nu]\, du \quad (25b)$$

$$\frac{\mu u_{n,z}}{a} = \frac{R\beta_1}{n}\int_0^{u_1} f''(\eta_1)\sinh u\sinh nu\, du + \frac{-R\beta_2^3}{n}\int_0^{u_2} g'''(\eta_2)\sinh u\sinh nu\, du \quad (25c)$$

Where $\eta_1 = Z - R\beta_1\cosh u$, $\eta_2 = Z - R\beta_2\cosh u$

And $f(\eta_1), g(\eta_2), h(\eta_2) = f_n(\eta_1), g_n(\eta_2), h_n(\eta_2)$ and primes represent the derivatives of the functions with respect to their arguments.

4. Boundary conditions

In order to satisfy the condition of a traction boundary at the face of the cavity, r=a, three of the stress components must satisfy the following boundary conditions:

$$\left.\begin{aligned}\sigma_{n,rr}\big]_{r=a} &= \sigma_{n1}u(Z)\\ \sigma_{n,rz}\big]_{r=a} &= \sigma_{n2}u(Z)\\ \sigma_{n,r\theta}\big]_{r=a} &= \sigma_{n3}u(Z)\end{aligned}\right\} \quad (26)$$

These equations are satisfied for each term n. The coefficients of the stress, $\sigma_{n,rr}, \sigma_{n,r\theta}$ and $\sigma_{n,rz}$ are expressed in equations (24) in integral form. These integrals include the unknown functions $f''(\eta_1), g'''(\eta_2)$ and $h''(\eta_2)$ which are to be found by solving the set of three simultaneous integral equations. These values then may be substituted back into the equations (24) and (25) to find the stress components and displacement components of the waves at any point on the boundary or in the medium behind the move front.

5. Solution of the Boundary Equations

Numerical solution of the boundary equations requires finding numerical values of the functions $f''(\eta_1), g'''(\eta_2)$ and $h''(\eta_2)$ .In the following paragraph, the changes in variables are used. At the boundary, the radius R is fixed, R=1. Therefore the arguments of the functions f'', g''' and h'' are:

$$\left.\begin{aligned}\eta_1 &= Z - \beta_1\cosh u\\ \eta_2 &= Z - \beta_2\cos hu\end{aligned}\right\} \quad (27)$$

$$\text{We let: } \xi_1 = \frac{Z}{\beta_1}, \quad \xi_2 = \frac{Z}{\beta_2} = k\xi_1 \quad (28)$$

Where $K = \beta_1/\beta_2$. Equations (27) may be written as:

$$\left.\begin{aligned}\eta_1 &= \beta_1(\xi_1 - \cosh u)\\ \eta_2 &= \beta_2(k\xi_1 - \cos hu)\end{aligned}\right.$$

A new variable ξ is now introduced by the following relations:

$$\left.\begin{aligned}\cosh u &= 1 + \xi\\ du &= \frac{d\xi}{\sin hu} = \frac{d\xi}{\sqrt{2\xi + \xi^2}}\end{aligned}\right\} \quad (29)$$

The limits of the integrals with this variable are as follows:

$$\text{Lower limits,} \quad u = 0 \quad , \xi = 0$$

$$\text{Upper limits} \begin{cases} u = u_1 & , \ \xi = \xi_1 \\ u = u_2 & , \ \xi = \xi_2 = k\xi_1 \end{cases} \qquad (30)$$

The upper limits are linear functions of Z and ξ_1 ; therefore, in order to perform numerical integration, the longitudinal axis ξ_1 is divided into small steps. At every point along this axis the numerical integration is performed and at each step only one new value of the functions $f''(\eta_1), g'''(\eta_2)$ and $h''(\eta_2)$ enters into the computations.

As an example of the procedure of the numerical integration, the component of the stress in the radial direction is given symbolically below:

$$\sigma_{n,rr} = I_{rr}^F + I_{rr}^G + I_{rr}^H \qquad (31)$$

Where

$$I_{rr}^F = \int_0^{u_1} f''(\eta_1)\left[M_2^2 - 2 + 2\beta_1^2 \sinh^2 u\right]\cosh nu\, du$$
$$I_{rr}^G = 2\beta_2^2 \int_0^{u_2} g'''(\eta_2)\cosh^2 u \cosh nu\, du \qquad (32)$$
$$I_{rr}^H = -\beta_2^2 \int_0^{u_2} h''(\eta_2)\sinh 2u \sinh nu\, du\, du$$

The integrals I_{rr}^F, I_{rr}^G and I_{rr}^H at the p^{th} step are expressed by using the convolution theorem in summation form as follows:

$$I_{rr}^F = \left(R_{rr}^{+F}\right)_0 (f)_p + \sum_{m=1}^{P-1} \left(R_{rr}^F\right)_m (f)_{P-m} + \left(R_{rr}^{-F}\right)_p (f)_0$$
$$I_{rr}^G = \left(R_{rr}^{+G}\right)_0 (g)_p + \sum_{m=1}^{P-1} \left(R_{rr}^G\right)_m (g)_{P-m} + \left(R_{rr}^{-G}\right)_p (g)_0 \qquad (33)$$
$$I_{rr}^H = \left(R_{rr}^{+H}\right)_0 (h)_p + \sum_{m=1}^{P-1} \left(R_{rr}^H\right)_m (h)_{P-m} + \left(R_{rr}^{-H}\right)_p (h)_0$$

Where (f), (g) and (h) are the unknown functions to be evaluated.

At this stage of integration the values $(f)_m$, $(g)_m$, $(h)_m$ are known for m=0 to p-1.The only unknowns in these expressions are $(f)_p$, $(g)_p$, and $(h)_p$. Similar expressions are written for the other components of stress, at the p^{th} step. The boundary conditions are now in the form of a set of three simultaneous linear equations. Solution of this set results in the values of $(f)_p$, $(g)_p$, and $(h)_p$. The procedure is then carried on to the $(P+1)^{th}$ step; Similar operations are performed to find the values of $(f)_{p+1}$, $(g)_{p+1}$, and $(h)_{p+1}$.

As mentioned previously, when the values f, g and h are found at each step, these values are substituted into the expressions for $u_{n,r}, u_{n,\theta}$ and $u_{n,z}$ $\sigma_{n,\theta\theta}, \sigma_{n,zz}, \sigma_{n,\theta z}$ to compute the numerical values of these stresses and displacements in the medium.

6. Numerical Results and Conclusion

For the non-axisymmetric loadings characterized by n > 0, numerical values of the stress components $\sigma_{n,\theta\theta}, \sigma_{n,zz}$ and $\sigma_{n,z\theta}$ at the cavity boundary r=a are presented in this section. These stresses are given for the cases n=1, 2 for each of the three step- traction loading indicated below:

Index	Applied load
K = 1	$\sigma_{rr}\big]_{r=a} = \sigma_{n1}\cos n\theta\, U(Z)$, $\sigma_{rz}\big]_{r=a} = \sigma_{r\theta}\big]_{r=a} = 0$
K = 2	$\sigma_{rz}\big]_{r=a} = \sigma_{n2}\cos n\theta\, U(Z)$, $\sigma_{rr}\big]_{r=a} = \sigma_{r\theta}\big]_{r=a} = 0$
K = 3	$\sigma_{r\theta}\big]_{r=a} = \sigma_{n3}\sin n\theta\, U(Z)$, $\sigma_{rr}\big]_{r=a} = \sigma_{rz}\big]_{r=a} = 0$

The curves are shown for two sets of prameters:

Case 1: $M_1 = \frac{V}{C_1} = 2 \quad ; \quad \upsilon = 0.25$

Case 2: $M_1 = \frac{V}{C_1} = 1.033 \quad ; \quad \upsilon = 0.25$

The values of M_1 were chosen for application of the results to problems of some practical interest. The stress components in each case approach the static plain strain solution as Z approaches infinity, indicating that mathematical model produces correct results for propagation of waves in the isotropic medium. For those cases in which the static solutions do not vanish, a typical overshoot above the value of the static (long term) solutions is observed. Moreover, a decrease in the Mach number M_1 appears to compress the stress response curve into a smaller range of Z such that the asymptotic values of the lower value M_1=1,033 are obtained for smaller values of Z. Figures 12 and 13 show the stress components $\sigma_{0,\theta\theta}$ and $\sigma_{0,zz}$ at the cavity boundary r=a for the axisymmetric loading case, n=0, for the mach numbers M_1=1.033, 1.5 and 2. As in the cases where $n \neq 0$, the stress components in each case approach the static plain solutions as Z approaches infinity. Figures 14 through 19 show the displacement components $u_{n,r}, u_{n,\theta}$ and $u_{n,Z}$ (n=1, 2, 3, 4) for each of the three loading cases, k=1, 2, 3. Figures 20 through 22 show the $u_{0,r}$ and $u_{0,Z}$ displacement components for the case n=0. These displacement results are shown for the M_1= 2, $\nu = 1/4$ case only.

The only property of the material in the medium which enters into computations is its poisson's ratio. Figures 23 through 26 represent the effect of this

parameter on the values of stress components for the axisymmetric loading case, n=0. The following values of poisson's ratio are used in this study:

$$\upsilon = 0 \ , 0.15, \ 0.25 \ \text{and} \ 0.35$$

It is noticed that the change in poisson's ratio does not have a large effect on the maximum value of longitudinal stress for the load case k=2 (Figure 26), while it affects considerably the value of longitudinal stress for the case load, k=1 (Figure 25), and hoop stress for the two cases, k=1,2 (Figures 23 and 24) for smaller values of Z.

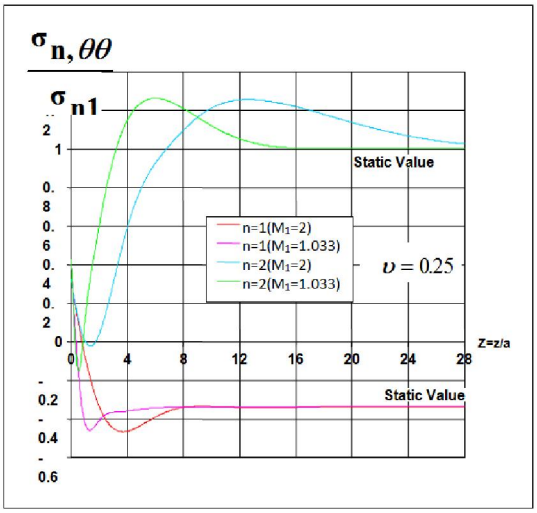

Figure 3. Stress $\sigma_{\theta\theta}$ at boundary due to step load; $\sigma_{rr} = \sigma_{n1}\cos n\theta u(Z); n = 1,2$

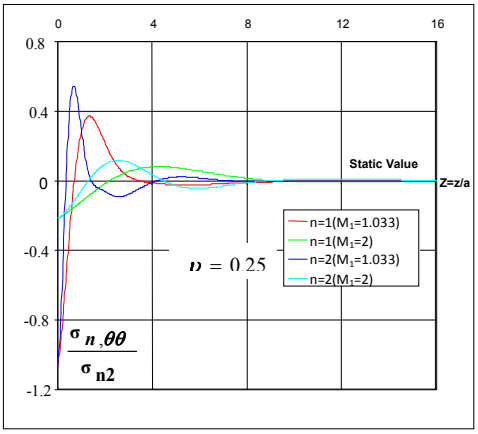

Figure 4. Stress $\sigma_{\theta\theta}$ at boundary due to step load: $\sigma_{rz} = \sigma_{n2}\cos n\theta u(Z); n = 1,2$

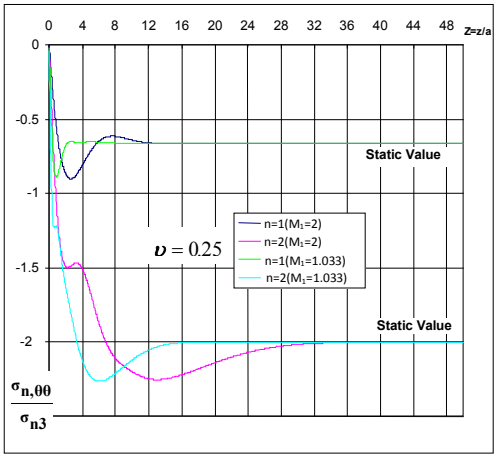

Figure 5. Stress $\sigma_{\theta\theta}$ at boundary due to step load; $\sigma_{r\theta} = \sigma_{n3}\sin n\theta u(Z); n = 1,2$

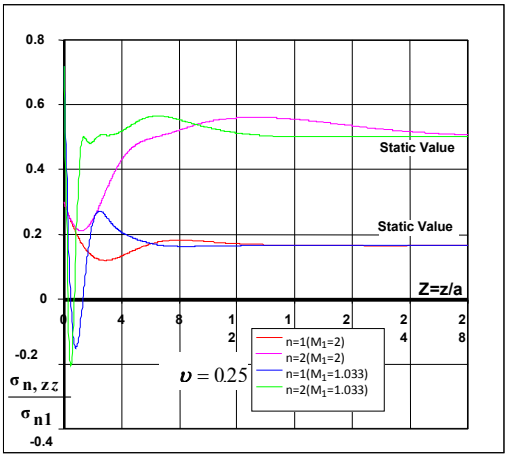

Figure 6. Stress σ_{zz} at boundary due to step load; $\sigma_{rr} = \sigma_{n1}\cos n\theta u(Z); n = 1,2$

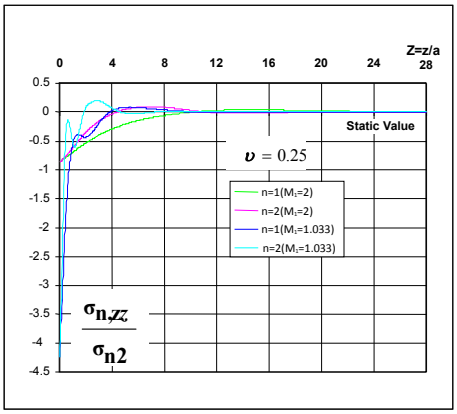

Figure 7. Stress σ_{zz} at boundary due to step load; $\sigma_{rz} = \sigma_{n2}\cos n\theta u(Z); n = 1,2$

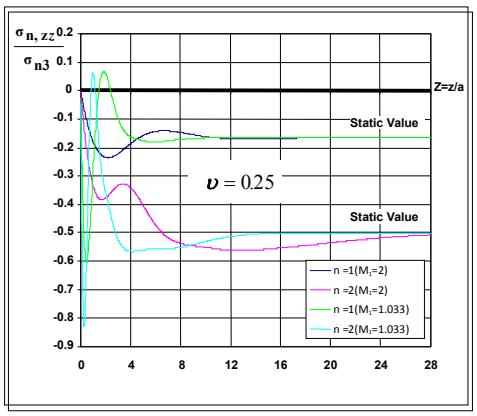

Figure 8. Stress σ_{zz} at boundary due to step load; $\sigma_{r\theta} = \sigma_{n3} \sin n\theta u(Z); n = 1,2$

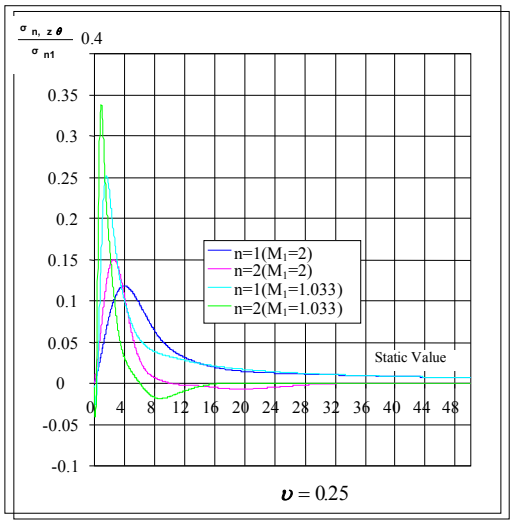

Figure 9. Stress $\sigma_{\theta z}$ at boundary due to step load; $\sigma_{rr} = \sigma_{n1} \cos n\theta u(Z); n = 1,2$

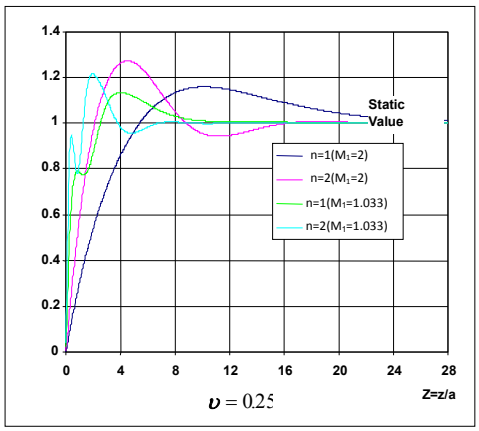

Figure 10. Stress $\sigma_{\theta z}$ at boundary due to step load; $\sigma_{rz} = \sigma_{n2} \cos n\theta u(Z); n = 1,2$

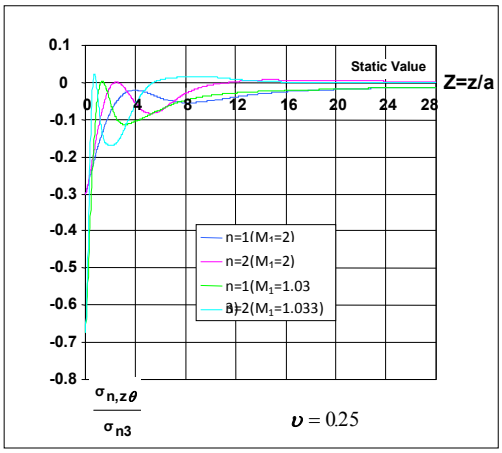

Figure 11. Stress $\sigma_{\theta z}$ at boundary due to step load; $\sigma_{r\theta} = \sigma_{n3} \sin n\theta u(Z); n = 1,2$

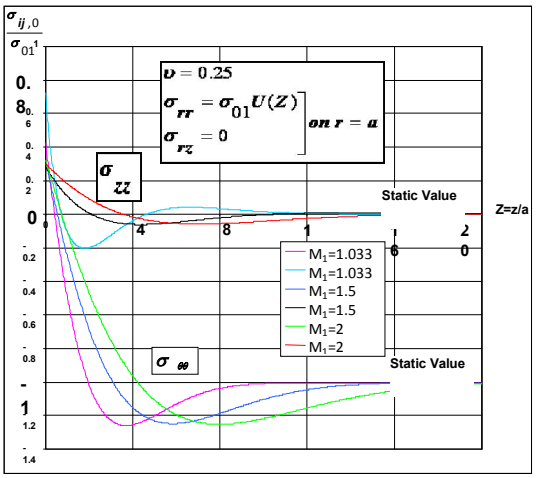

Figure 12. Stresses at boundary due to axisymmetric step load $\sigma_{rr} = \sigma_{n1} u(Z); n = 0$

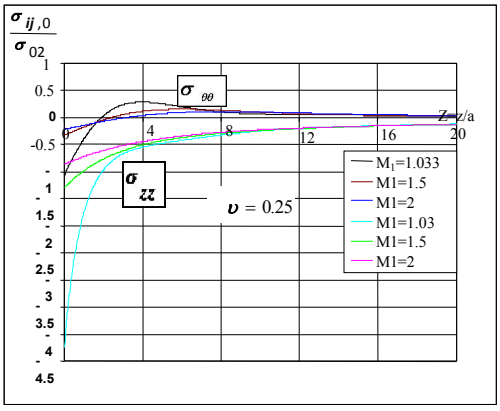

Figure 13. Stresses at boundary due to axisymmetric step load $\sigma_{rz} = \sigma_{n2} u(Z); n = 0$

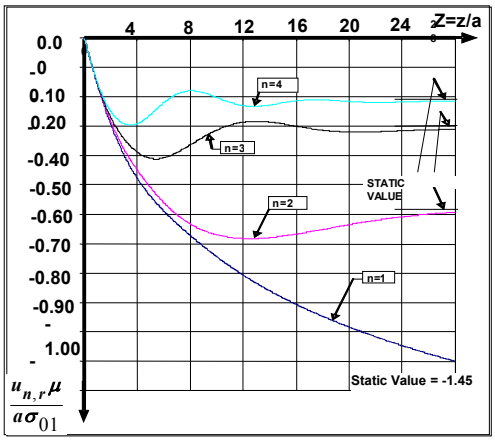

Figure 14. Boundary displacement $u_{n,r}$ due to step load $\sigma_{rr} = \sigma_{n1}\cos n\theta\, u(Z); n = 1,2,3,4$, $M_1 = 2$, $\upsilon = 0.25$,

$\sigma_{r\theta} = \sigma_{rz} = 0$

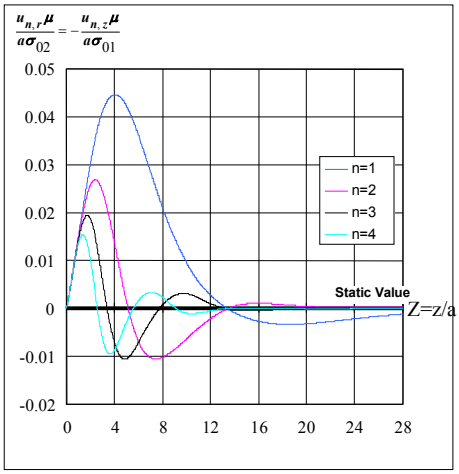

Figure 15. Boundary displacements due to step load;n=1,2,3,4 , $M_1 = 2$, $\upsilon = 0.25$

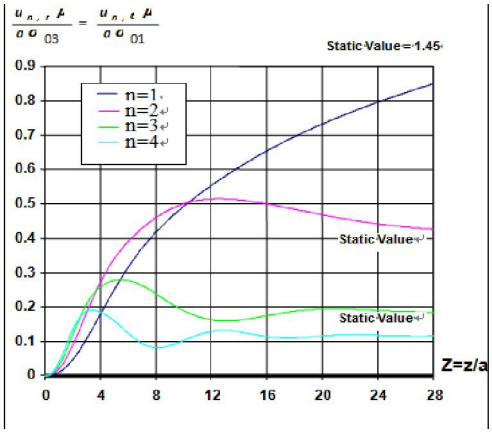

Figure 16. Boundary displacements due to step load;n=1,2,3,4 , $M_1 = 2$, $\upsilon = 0.25$

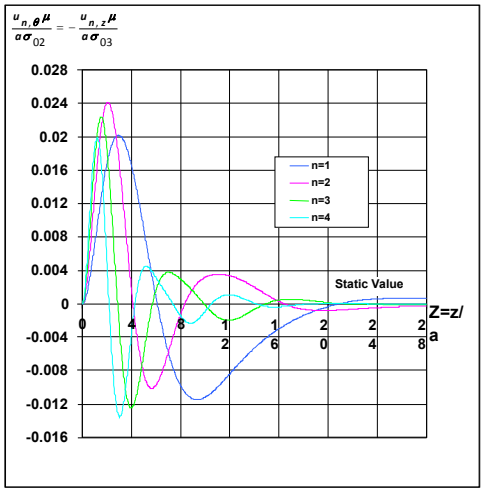

Figure 17. Boundary displacements due to step load;n=1,2,3,4 , $M_1 = 2$, $\upsilon = 0.25$

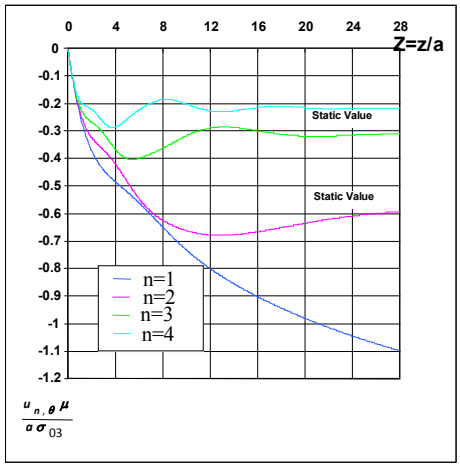

Figure 18. Boundary displacements due to step load;n=1,2,3,4 , $M_1 = 2$, $\upsilon = 0.25$

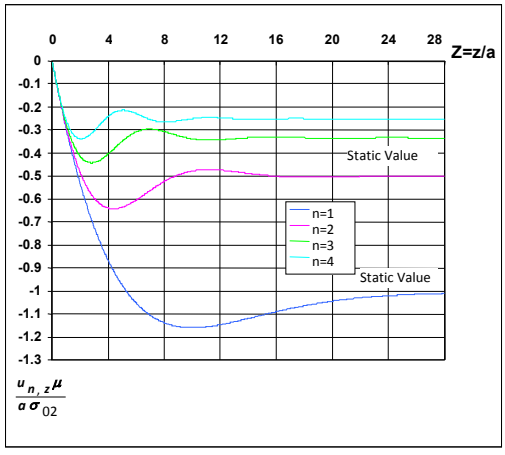

Figure 19. Boundary displacements due to step load;n=1,2,3,4 , $M_1 = 2$, $\upsilon = 0.25$

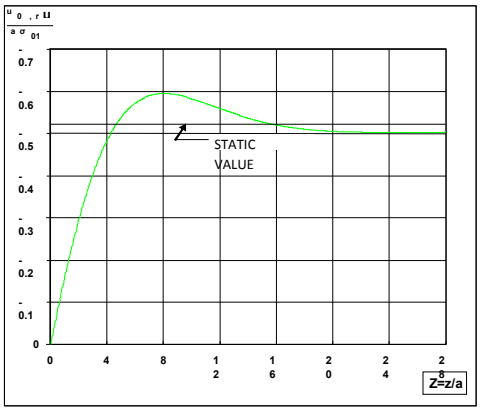

Figure 20. Boundary displacement $u_{0,r}$ due to step load σ_{01}; n=0 , $M_1 = 2$, $\upsilon = 0.25$

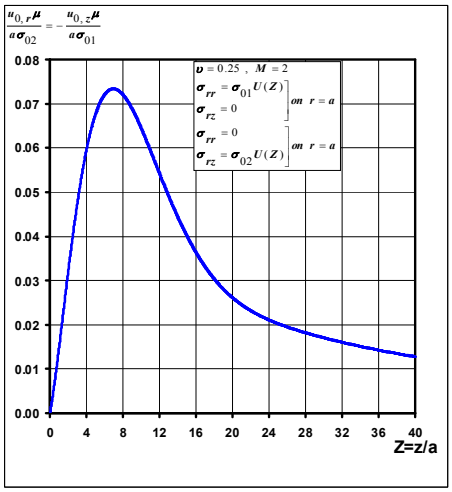

Figure 21. Boundary displacement $u_{0,r}$ due to step load σ_{02}; n= 0 $u_{0,z}$ due to step load σ_{01}; n= 0 , $M_1 = 2$, $\upsilon = 0.25$

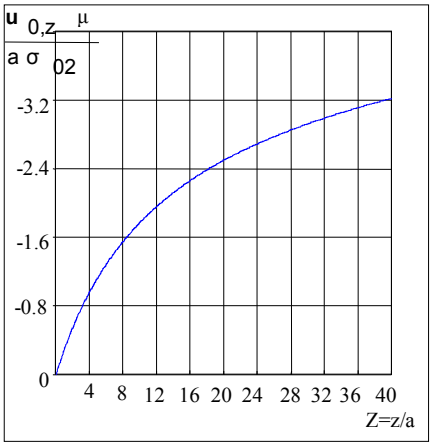

Figure 22. Boundary displacement $u_{0,z}$ due to step load σ_{02}; n= 0

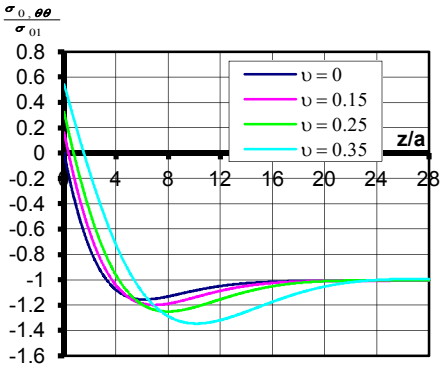

Figure 23. Comparision of Hoop stress for different values of poisson's ratio at boundary r=a due to axisymmetric step load σ_{01}; n= 0,M_1=2

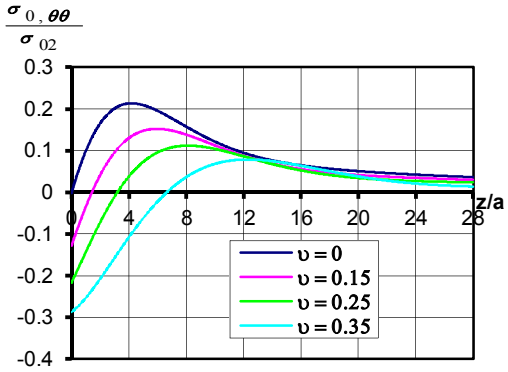

Figure 24. Comparision of Hoop stress for different values of poisson's ratio at boundary r=a due to axisymmetric step load σ_{02}; n= 0,M_1=2

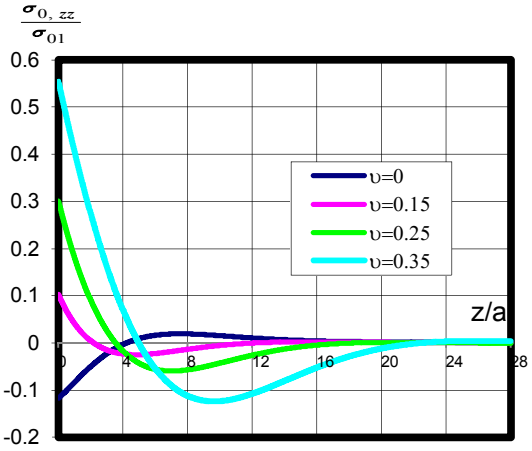

Figure 25. Comparision of Longitudinal stress for different values of poisson's ratio at boundary r=a due to axisymmetric step load σ_{01}; n= 0, M_1=2

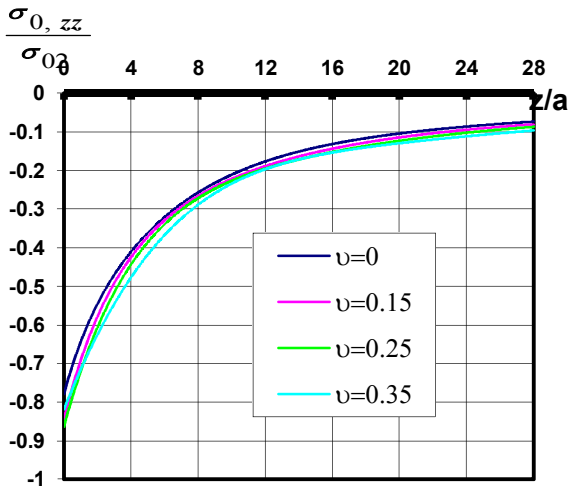

Figure 26. Comparision of Longitudinal stress for different values of poisson's ratio at boundary r=a due to axisymmetric step load σ_{02}; n= 0, M_1=2

Appendix A

Verification of the Solution of Wave Equation

Consider the modified wave equations expressed in equations (20). A typical differential equation of this kind is expressed as:

$$\nabla^2\varphi = M^2\varphi_{zz}$$

Or

$$-\alpha^2\varphi_{ZZ} + \varphi_{RR} + \frac{1}{R}\varphi_R - \frac{n^2}{R^2}\varphi = 0 \qquad (A.1)$$

A solution of this differential equation was represented in the following form.

$$\varphi = \int_0^{u_1} f(Z - R\beta\cosh u)\cosh nu\, du \qquad (A.2)$$

Where

$$u_1 = \cosh^{-1}(1 + \frac{Z}{R\beta})$$

In this section, the solution (A.2) is checked by substitution of φ into equation (A.1).

Partial derivatives of φ are:

$$\varphi_R = -\beta\int_0^{u_1} f'(\eta)\cosh u\cosh nu\, du$$

$$\varphi_{RR} = \beta^2\int_0^{u_1} f''(\eta)\cosh^2 u\cosh nu\, du \qquad (A.3)$$

$$\varphi_{ZZ} = \int_0^{u_1} f''(\eta)\cosh nu\, du$$

Where

$$\eta = Z - R\beta\cosh u$$

The function φ may be integrated by parts as follows:

$$\varphi = \int_0^{u_1} f(\eta)\cosh nu\, du = \frac{1}{n}f(\eta)\sinh nu\Big|_0^{u_1} + \frac{R\beta}{n}\int_0^{u_1} f'(\eta)\sinh u\sinh nu\, du \qquad (A.4)$$

The first term on the right hand side is zero, since $f(\eta)$ is zero for values of u greater than u_1. In a similar manner φ_R can be integrated by parts,

$$\varphi_R = -\beta\int_0^{u_1} f'(\eta)\cosh nu\cosh u\, du$$

$$\varphi_R = -R\beta^2\int_0^{u_1} f''(\eta)\sinh^2 u\cosh nu\, du + n\beta\int_0^{u_1} f'(\eta)\sinh u\sinh nu\, du$$

It is easily seen that substitution of the values φ, φ_R, φ_{RR} and φ_{ZZ} into equation (A.1) satisfies this equation.

Similar solutions are obtained for the functions ψ and χ.

References

1. Biot MA. Propagation of Elastic Waves in a cylindrical Bore containing a fluid. Applied physics 1952; 23(9):997-1005.
2. Cole J, Huth J. Stresses produced in a Half-plane by Moving loads. Applied Mechanics 1958; 25(4):699-704.
3. Iavorskaia IM. Diffraction of a plane Longitudinal wave on Circular Cylinder. Doklady, akad. Nauk USSR 1964; 158(6).
4. Baltrukonis JH, Gottenberg WG, Schreiner RN. Dynamics of a Hollow Elastic cylinder Contained by an Infinitely Long Rigid Circular Cylinrical Tank. the Acoustical Society of America 1960; 32(12):1539-1546.
5. Forrestal MJ, Herrman G. Response of a Submerged Cylindrical Shell to an Axially Propagating Step Wave. Applied Mechanics 1965;32(4):788-792.
6. Biot MA. Theory of propagation of elastic waves in fluid-saturated porous solid. Acoustic Soc. 1956; 28(2):168-191.
7. Henrych J. The dynamics of explosion and its use. New York, Elsevier, 1956; 576.
8. Wong KC, Shah AH, Datta SK. Dynamic Stresses and Displacements in Buried Tunnel. Journal of Engineering Mechanics 1985; 111(2):218–234.

9. Achenbach JD. Wave Propagation in Elastic Solids. North-Holland, New York 1973; 425.
10. Gregory RD. An Expansion Theorem Applicable to Problems of Wave Propagation in an Elastic Half-Space Containing a Cavity. Mathematical Proceedings of the Cambridge Philosophical Society 1967; 63(4):1341−1367.
11. Gregory RD. The Propagation of Waves in an Elastic Half-Space Containing a Cavity. Mathematical Proceedings of the Cambridge Philosophical Society 1970; 67(3): 689−709.
12. De-Hoop AT. The moving-load problem in soil dynamics-the vertical displacement approximation. Wave Motion 2002;36: 335-346.
13. Aliakbarian M. Oblique incidence of plane stress waves on a circular tunnel. Ph. D. Thesis, University of Illinois at Urbana, Illinois 1967.
14. Rahman, M. Fourier-Transform Solution to the problem of steady-state Transonic motion of a line load across the surface of an elastic Half-Space. Applied Mathematics Letters 2001; 14(4): 437-441.
15. Bakker MCM, Verweij MD, Kooij BJ, Dieterman HA. The traveling point load revisited. J Wave Motion 1999; 29(2):119-135.

9/17/2015